

# Dalton Transactions

Accepted Manuscript



This is an *Accepted Manuscript*, which has been through the Royal Society of Chemistry peer review process and has been accepted for publication.

*Accepted Manuscripts* are published online shortly after acceptance, before technical editing, formatting and proof reading. Using this free service, authors can make their results available to the community, in citable form, before we publish the edited article. We will replace this *Accepted Manuscript* with the edited and formatted *Advance Article* as soon as it is available.

You can find more information about *Accepted Manuscripts* in the [Information for Authors](#).

Please note that technical editing may introduce minor changes to the text and/or graphics, which may alter content. The journal's standard [Terms & Conditions](#) and the [Ethical guidelines](#) still apply. In no event shall the Royal Society of Chemistry be held responsible for any errors or omissions in this *Accepted Manuscript* or any consequences arising from the use of any information it contains.

## ARTICLE

# Facile redox state manipulation in Cu(I) frameworks by utilisation of the redox-active tris(4-(pyridin-4-yl)phenyl)amine ligand

Cite this: DOI: 10.1039/x0xx00000x

Carol Hua,<sup>a</sup> Peter Turner<sup>a</sup> and Deanna M. D'Alessandro\*<sup>a</sup>Received 00th January 2012,  
Accepted 00th January 2012

DOI: 10.1039/x0xx00000x

www.rsc.org/

The incorporation of a redox-active tris(4-(pyridine-4-yl)phenyl)amine (NPY<sub>3</sub>) ligand into the Cu(I) coordination frameworks [CuNPY<sub>3</sub>NO<sub>3</sub>.solvent]<sub>n</sub> and [CuNPY<sub>3</sub>Cl.solvent]<sub>n</sub> has been shown to facilitate redox state switching in the materials. In both cases, the initial Cu(II) metal centre was reduced *in situ* during the solvothermal synthesis under relatively mild conditions where the use of chloride and nitrate counterions resulted in significantly different structures. Solid state electrochemical and Vis/NIR spectroelectrochemical experiments facilitated the characterisation and manipulation of the accessible redox states, demonstrating the highly tunable nature of the spectral properties – a property of significant interest in the design of advanced materials.

## Introduction

Multifunctional coordination solids in which more than one property coexists are gaining increasing attention in the development of advanced functional materials.<sup>[1]</sup> In particular, coordination frameworks are ideal candidates for exploring deeply fundamental aspects of multifunctionality in 3-dimensional coordination space due to the control afforded over their properties by systematic alteration of the electronic, magnetic and structural characteristics of the components.<sup>[2-7]</sup> The potential to subtly and systematically vary the ligand and metal ions in framework syntheses allows the porosity, thermal and chemical robustness of the materials to be optimally tuned for use in a variety of applications where external stimuli such as an electrochemical potential, or exposure to light irradiation can be used to 'trigger' a change in framework properties.<sup>[6-9]</sup>

Metal-Organic Frameworks (MOFs) provide a versatile platform for the development of multifunctional materials, however, their electroactive properties<sup>[10]</sup> have been reported in relatively few cases. Nevertheless, framework materials possess interesting magnetic and electronic properties<sup>[11]</sup> which are highly relevant to their potential applications as porous conductors,<sup>[12-14]</sup> catalysts<sup>[15-18]</sup> and chemical sensors,<sup>[10]</sup> amongst others.

In this regard, tris(4-(pyridin-4-yl)phenyl)amine (NPY<sub>3</sub>) represents an appealing ligand for the synthesis of multifunctional redox-active materials, and has previously been incorporated into a number of coordination frameworks and

MOFs with Cu(II),<sup>[8, 19]</sup> Cu(I)<sup>[20]</sup> and Mn(II)<sup>[9]</sup> in addition to Cd(II),<sup>[21-23]</sup> Co(II),<sup>[19, 21-22]</sup> Zn(II),<sup>[19, 22]</sup> and Ni(II)<sup>[21]</sup> metal ions with dicarboxylate coligands. These frameworks were primarily investigated for their structural characteristics<sup>[19-21]</sup> with limited attention focused on their electrochemical and spectral properties.<sup>[8-9]</sup>

Herein, we report the syntheses, crystal structures and redox-activity of two Cu(I) frameworks, [CuNPY<sub>3</sub>Cl.solvent]<sub>n</sub> and [CuNPY<sub>3</sub>NO<sub>3</sub>.solvent]<sub>n</sub>, in which the Cu(I) centres have been generated via *in situ* reduction of Cu(II) ions. The different redox states present in the frameworks have been accessed through *in situ* solid state spectroelectrochemical and *ex situ* chemical oxidation experiments to interrogate the dependence of the optical properties on the redox states of the materials. The electroactivity of these materials underscores their potential as attractive platforms for the design of multifunctional coordination solids.

## Results and Discussion

The two Cu(I) frameworks containing the NPY<sub>3</sub> ligand were synthesised with Cu(II) salts by solvothermal methods in either DMF ([CuNPY<sub>3</sub>NO<sub>3</sub>.solvent]<sub>n</sub>) or a mixture of DMF and MeOH ([CuNPY<sub>3</sub>Cl.solvent]<sub>n</sub>). The *in situ* reduction of Cu(II) to Cu(I) by pyridyl ligands under solvothermal processes is well-known, with several reports having appeared in the literature for Cu(NO<sub>3</sub>)<sub>2</sub>,<sup>[24-26]</sup> Cu(SO<sub>4</sub>)<sub>2</sub>,<sup>[27]</sup> CuCl<sub>2</sub><sup>[28]</sup> and CuO salts.<sup>[29]</sup> In all cases, temperatures above 140 °C were required.

The synthesis of  $[\text{CuNPy}_3\text{Cl}\cdot\text{solvent}]_n$  was achieved by heating the  $\text{NPy}_3$  ligand with  $\text{CuCl}_2$  in a 1:1 mixture of DMF and MeOH at 130 °C for 4 days to obtain the framework as bright orange needles. The solid state structure was determined using single crystal X-ray diffraction and found to be isostructural with an analogue synthesised directly from  $\text{CuBr}$ .<sup>[20]</sup> The core of the monoclinic  $[\text{CuNPy}_3\text{Cl}\cdot\text{solvent}]_n$  structure is dinuclear with  $\mu$ -chloro ligands bridging paired Cu(I) centres 2.6425(9) Å apart (Fig. 1a). The copper to chloride distance is 2.4777(9)Å, a distance consistent with the two  $\mu$ -chloro four coordinate Cu(I) complexes in the current release of the Cambridge Structural Database.<sup>[30]</sup> The Cu(I) tetrahedral coordination sphere is slightly distorted, evidently reflecting hindrance from phenyl groups (N1-Cu1-N2: 117.37(10)°, N1-Cu1-Cl1: 99.74(7)°, Cl1-Cu1-Cl1: 113.37(3)°, N2-Cu1-Cl1: 110.85(8)°). The phenyl rings present in the  $\text{NPy}_3$  ligand are tilted in a propeller-like conformation about the central nitrogen atom, consistent with previously reported solid state structures of triarylamine systems.<sup>[31]</sup>

The  $[\text{CuNPy}_3\text{Cl}\cdot\text{solvent}]_n$  framework contained a series of (4,4)-nets, where a single network consisted of a distorted 2D diamondoid-type shape (Fig. 1b). These individual networks were interpenetrated with each other to form a 3D structure where channels can be observed down the  $c$  axis (Fig. 1c) and feature uncoordinated pyridyl  $N$ -donors from one arm of the  $\text{NPy}_3$  ligand which extend into the pore space (Fig. 1c). The presence of the uncoordinated pyridyl  $N$ -donor opens up the possibility of post-synthetic modification of the framework where extra substituents could be introduced to coordinate to this  $N$ -donor. The framework contained a pair of left and right-handed 1D helical channels that were alternately arranged within the material. The use of the SQUEEZE function in Platon revealed a void space of 23.2%.<sup>[32]</sup> The thermal gravimetric analysis showed that the framework was stable up to 300 °C with the weight loss below 150 °C corresponding to the loss of solvent molecules, methanol and DMF, from the pores (ESI).

The  $[\text{CuNPy}_3\text{NO}_3\cdot\text{solvent}]_n$  framework was synthesised by heating  $\text{NPy}_3$  with  $\text{Cu}(\text{NO}_3)_2\cdot 3\text{H}_2\text{O}$  in DMF overnight at 80 °C to yield yellow prismatic crystals. Surprisingly mild conditions compared to previous reports<sup>[24-26]</sup> were required for the *in situ* reduction of Cu(II) to Cu(I) using  $\text{Cu}(\text{NO}_3)_2\cdot 3\text{H}_2\text{O}$ . This may reflect the presence of the  $\text{NPy}_3$  ligand, which can act as a reducing agent in being oxidised to form the triarylamine radical cation. The crystals obtained from the synthesis were suitable for single crystal X-ray diffraction analysis.

The asymmetric unit of the orthorhombic structure model includes a nitrate ion half occupying two sites, with one bound to the metal at the apical trigonal pyramidal coordination site of an otherwise three-coordinate copper ion (Fig. 2a). The second nitrate site is effectively non-coordinating and is located *trans* to the apical coordination site, with the closest nitrate oxygen to copper ion distance being 3.978(8)Å. The coordinated pyridyl residues appear to prevent coordination, with the nitrate oxygen closest to the copper having pyridyl hydrogen distances of 2.475 and 2.679Å.

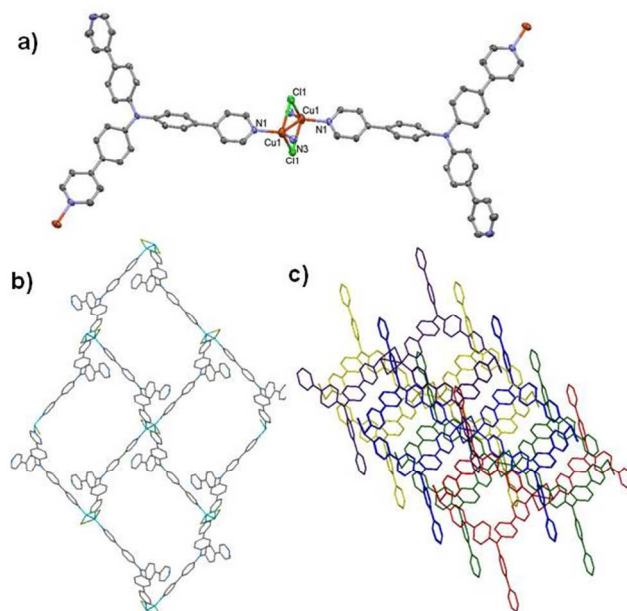


Fig. 1 Solid state structure of  $[\text{CuNPy}_3\text{Cl}\cdot\text{solvent}]_n$  showing a) coordination sphere around the Cu(I) centre, b) one network along the  $c$  axis showing diamond-shaped nets and c) interpenetrated networks along the  $b$  axis.

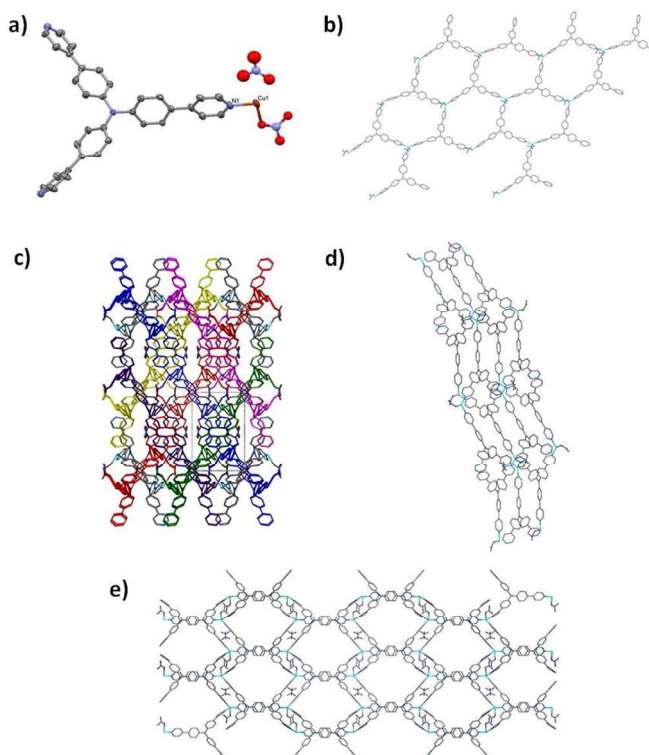


Fig. 2 Solid state structure of  $[\text{CuNPy}_3\text{NO}_3\cdot\text{solvent}]_n$  showing a) asymmetric unit, b) one 2D network, c) interwoven 2D networks to form the 3D structure, d) view along the  $c$  axis and e) view along the  $a$  axis.

Full occupancy of the apical coordination site in  $[\text{CuNPy}_3\text{NO}_3\cdot\text{solvent}]_n$  is prevented by the proximity of the

copper ion of a neighbouring complex molecule. The copper-copper distance is 6.4227(17)Å, which is not close enough for the nitrate ion to bridge the two metal centres. The closest of the two non-coordinated oxygen atoms of the coordinated nitrate is 3.467(7)Å from the nearby three coordinate metal centre. The structure is then a 50:50 mixture of three and four coordinate copper complexes.

The angles formed between the coordinated pyridyl nitrogen atoms and the copper centre deviate from 120°, with the N1-Cu1-N2 angle being 132.37(14)°, N1-Cu1-N3 being 121.15(13)° and N2-Cu1-N3 being 99.21(14)°. The coordination bond lengths are consistent with other four coordinate Cu(I) complexes having apical oxygen atoms and approximately trigonal pyramid coordination. The copper-nitrogen distances are 1.946(3), 1.975(3) and 2.039(3) Å, and the copper-oxygen distance is 2.423(5)Å. Perhaps reflecting the admixed coordination, the Cu displacement ellipsoid is slightly elongated in the direction of the nearest oxygen atom of the non-coordinated nitrate ion.

The framework consists of a series of 2D (6,3)-nets which formed a honeycomb-type structure (Fig. 2b). The 2D layers interpenetrate each other in an inclined manner to form a 3D material (Fig. 2c). The framework appeared as a wave-like structure when viewed down the *c* axis (Fig. 2e) whilst large pores throughout the structure can be observed down the *a* axis (Fig. 2d).

### Electrochemical Properties

Solid state cyclic voltammograms were conducted in  $[(n-C_4H_9)_4N]PF_6/CH_3CN$  electrolyte on the two copper frameworks to elucidate their redox properties (Fig. 3). The cyclic voltammogram of  $[CuNPY_3Cl.solvent]_n$  exhibited a *quasi* reversible anodic process at 0.8 V vs.  $Fc/Fc^+$  which was assigned to the one electron oxidation of the Cu(I) centre to Cu(II) (Fig. 3a). The broadness of this peak may either suggest that the two Cu(I) centres in the framework, linked by chloride ligands, oxidise at similar potentials such that the individual anodic waves due to each of the centres are not fully distinguishable or be due to the effects of counterion diffusion into the pores of the framework material. This was supported by the increasing peak-width at half-height of the anodic signal at slower scan rates. The irreversible cathodic process at -1.5 V vs.  $Fc/Fc^+$  was assigned to reduction of the Cu(II) metal centre formed during the oxidative process to the original Cu(I) species.

One major anodic process was observed for the  $[CuNPY_3NO_3.solvent]_n$  framework, where the oxidation of the triarylamine core and Cu(I) occurred at similar potentials of *ca.* 0.89 V vs.  $Fc/Fc^+$  (Fig. 3b). Reduction of the Cu(II) formed during the anodic scan was observed at -2.25 V vs.  $Fc/Fc^+$  at fast scan rates (500 mV/s); at slower scan rates (100 and 200 mV/s), the Cu(II) species formed appears to decompose due to the longer time-scale of the experiments.

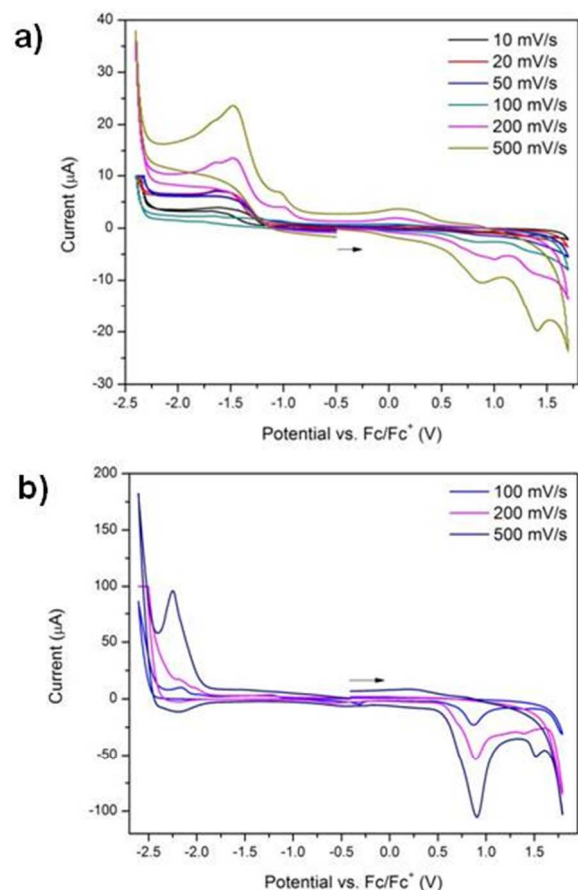


**Fig. 3** Solid state electrochemistry in  $[(n-C_4H_9)_4N]PF_6/CH_3CN$  electrolyte of the a)  $[CuNPY_3Cl.solvent]_n$  framework with scan rates of 10 to 500 mV/s and b)  $[CuNPY_3NO_3.solvent]_n$  framework at scan rates of 100, 200 and 500 mV/s.

### Spectral Properties and Chemical Oxidation

Similar spectral properties were observed for the two frameworks which lacked any significant bands in the Vis/NIR region due to the presence of the  $d^{10}$  Cu(I) centres (Fig. 4). The bands at 20880  $cm^{-1}$  (479 nm) for  $[CuNPY_3Cl.solvent]_n$  and at 22150  $cm^{-1}$  (452 nm) for  $[CuNPY_3NO_3.solvent]_n$  were assigned to a MLCT process from the Cu(I) centre to the triarylamine core of the ligand. These charge-transfer process were responsible for the bright orange ( $[CuNPY_3Cl.solvent]_n$ ) and yellow ( $[CuNPY_3NO_3.solvent]_n$ ) colouration of the frameworks, which otherwise were expected to be pale coloured.<sup>[33]</sup> The bands at energies above 25000  $cm^{-1}$  (400nm) originate predominantly from  $\pi$  to  $\pi^*$  transitions of the triarylamine core.<sup>[34]</sup>

Over the period of one week, the colour change observed from orange to green for the  $[CuNPY_3Cl.solvent]_n$  framework was ascribed to auto-oxidation of the Cu(I) centre to Cu(II) by atmospheric oxygen. The oxidation of Cu(I) was presumably accompanied by a rearrangement in the coordination sphere of the metal centre, as distorted tetrahedral Cu(II) complexes typically appear orange.<sup>[33]</sup> As the Cu(II) centre possesses a

lower electron density than Cu(I), the MLCT band at  $20300\text{ cm}^{-1}$  ( $493\text{ nm}$ ) was blue shifted to  $22160\text{ cm}^{-1}$  ( $451\text{ nm}$ ) due to the higher energy required for the MLCT process. Upon auto-oxidation of the  $[\text{CuNPY}_3\text{Cl}\cdot\text{solvent}]_n$  framework in air and the formation of a green coloured material, two bands appeared in the NIR region at  $9620$  ( $1040\text{ nm}$ ) and  $13270\text{ cm}^{-1}$  ( $754\text{ nm}$ ) and were assigned to  $d-d$  transitions of the  $d^9$  Cu(II) centre (Fig. 4).<sup>[33]</sup>

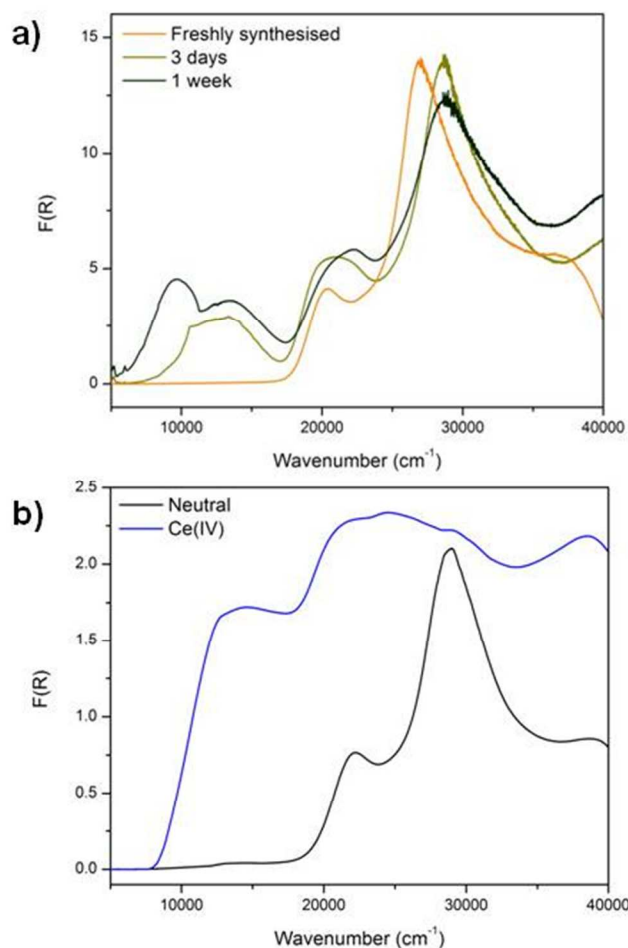


Fig. 4 Solid state UV/Vis/NIR spectra of the a)  $[\text{CuNPY}_3\text{Cl}\cdot\text{solvent}]_n$  and b)  $[\text{CuNPY}_3\text{NO}_3\cdot\text{solvent}]_n$  frameworks over the range  $5000\text{--}40000\text{ cm}^{-1}$  ( $250\text{--}2000\text{ nm}$ ) and their oxidised analogues.

Chemical oxidation of the  $[\text{CuNPY}_3\text{NO}_3\cdot\text{solvent}]_n$  framework was attempted *ex situ* with Ce(IV) (Fig. 4). The use of this oxidant resulted in a significant red shift of the lowest energy band at  $22000\text{ cm}^{-1}$  ( $455\text{ nm}$ ) and the formation of a band at  $13300\text{ cm}^{-1}$  ( $752\text{ nm}$ ) which was assigned to the  $\pi$  to  $\pi^*$  transition of the triarylamine radical cation in the ligand and was in good agreement with the spectral properties of previously reported radical cation triarylamine species.<sup>[34]</sup> The additional higher energy bands above  $20000\text{ cm}^{-1}$  ( $500\text{ nm}$ ) are due to charge transfer transitions of the Cu(II) centre which was oxidised concurrently with the triarylamine core in accord with the electrochemical measurements. Chemical oxidation of the  $[\text{CuNPY}_3\text{NO}_3\cdot\text{solvent}]_n$  framework led to both oxidation of the

Cu(I) centre and the triarylamine core which contrasted with the results from auto-oxidation in air of the  $[\text{CuNPY}_3\text{Cl}\cdot\text{solvent}]_n$  framework where only oxidation of the Cu(I) centre was observed.

### Solid State Vis/NIR Spectroelectrochemistry

To verify the formation of the triarylamine radical cation as observed upon chemical oxidation with Ce(IV), an *in situ* solid state spectroelectrochemical experiment in  $[(n\text{-C}_4\text{H}_9)_4\text{N}]\text{PF}_6/\text{CH}_3\text{CN}$  electrolyte was performed (Fig. 5).<sup>[35]</sup> Upon application of a positive potential, a slight darkening of the sample from bright yellow to dark yellow was observed which corresponded to the appearance of a broad band at  $13800\text{ cm}^{-1}$  ( $725\text{ nm}$ ). This band was indicative of successful oxidation of the triarylamine core and was assigned to the  $\pi$  to  $\pi^*$  (or  $D_0$  to  $D_1$ ) transition of the triarylamine radical cation. The band at  $13800\text{ cm}^{-1}$  ( $725\text{ nm}$ ) obtained during the solid state spectroelectrochemical experiment corresponds well with that observed upon chemical oxidation of the framework with Ce(IV). The increase in the intensity of the band at  $23000\text{ cm}^{-1}$  ( $435\text{ nm}$ ) is consistent with the concurrent oxidation of Cu(I) to form Cu(II).

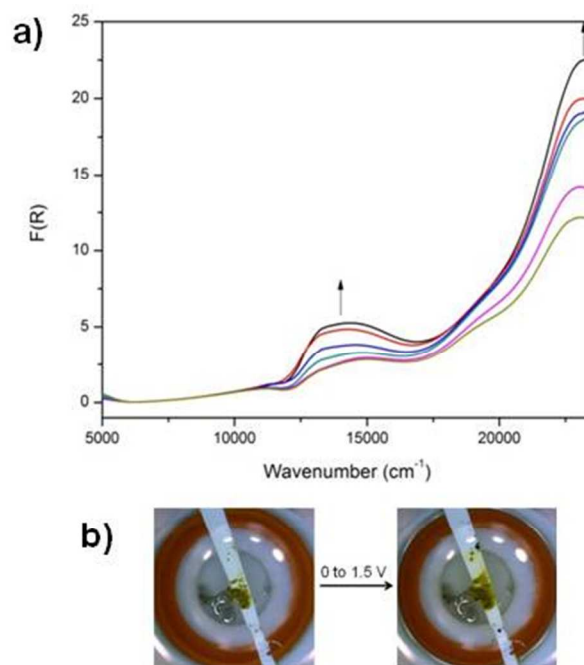


Fig. 5 Solid state *in situ* spectroelectrochemistry on the  $[\text{CuNPY}_3\text{NO}_3\cdot\text{solvent}]_n$  framework in  $[(n\text{-C}_4\text{H}_9)_4\text{N}]\text{PF}_6/\text{CH}_3\text{CN}$  electrolyte a) upon increasing the potential from 0 to 1.5 V and b) photos of the framework during the experiment.

## Conclusions

The incorporation of a redox-active triarylamine ligand,  $\text{NPY}_3$ , into coordination frameworks can be exploited to facilitate facile redox state switching. In the present case, two Cu(I) frameworks were synthesised with the  $\text{NPY}_3$  ligand from Cu(II)

salts to yield  $[\text{CuNPY}_3\text{Cl}\cdot\text{solvent}]_n$  and  $[\text{CuNPY}_3\text{NO}_3\cdot\text{solvent}]_n$ . The differences in the solid state structures of the two frameworks presumably resulted from the different Lewis acidity of the chloride and nitrate counterions used. The electrochemical properties of these frameworks were elucidated to demonstrate the facile manipulation of the electroactive components in the frameworks. The different properties obtainable through application of a chemical or electrochemical stimulus offer exciting prospects for application of these frameworks as multifunctional materials where the functional characteristics are able to be controlled through redox-state switching.

## Experimental

### General Considerations

Distilled and degassed acetonitrile (dried over  $\text{CaH}_2$ ) was used for all electrochemical experiments. DMF was dried over activated  $\text{CaSO}_4$  then distilled under reduced pressure. Methanol was distilled over  $\text{Mg/I}_2$ . Microanalyses were carried out at the Chemical Analysis Facility – Elemental Analysis Service in the Department of Chemistry and Biomolecular Science at Macquarie University, Australia. The tris(4-(pyridin-4-yl)phenyl)amine ( $\text{NPY}_3$ ) ligand was synthesised according to literature procedures.<sup>[8-9]</sup>

### Synthesis of Frameworks

**$[\text{CuNPY}_3\text{NO}_3\cdot\text{solvent}]_n$  framework.** The  $\text{NPY}_3$  ligand (11.2 mg,  $2.35 \times 10^{-5}$  mol) and  $\text{Cu}(\text{NO}_3)_2\cdot 3\text{H}_2\text{O}$  (17.0 mg,  $7.05 \times 10^{-5}$  mol) were suspended in DMF (1 mL) and heated to 80 °C for 18 hours. The initially green suspension became a green solution before yellow prismatic crystals were formed (9.5 mg, 73%). Elemental analysis: Found C, 56.66; H, 5.94; N, 11.62. Calculated for  $\text{C}_{40}\text{H}_{40}\text{CuN}_6\text{O}_{10}\cdot 2.06\text{DMF}$ : C, 56.66; H, 5.60 and N, 11.53%

**$[\text{CuNPY}_3\text{Cl}\cdot\text{solvent}]_n$  framework.** The pyridyl ligand (22.8 mg,  $4.78 \times 10^{-5}$  mol) and  $\text{CuCl}_2\cdot 2\text{H}_2\text{O}$  (24.0 mg,  $1.44 \times 10^{-4}$  mol) were suspended in a mixture of distilled DMF (1 mL) and methanol (1 mL). The mixture was heated at 10 °C/min to 130 °C in a Parr bomb for 96 hours and then cooled at a rate of 0.1 °C/min to room temperature to yield large orange needles. These crystals were washed quickly with methanol before being dried (18 mg, 66%). Elemental analysis: Found C, 61.41; H, 6.67 and N, 9.01; Calculated for  $\text{C}_{33}\text{H}_{24}\text{ClCuN}_4\cdot 4.31\text{MeOH}\cdot 1.11\text{DMF}$ : C, 61.41; H, 6.22 and N, 9.01%

**Chemical Oxidation using Ce(IV).** A solution of ammonium cerium nitrate in water was added to a suspension of the framework in water. The reaction was stirred for 10 mins before the solid was filtered and washed with water.

### Crystallography

**$[\text{CuNPY}_3\text{Cl}\cdot\text{solvent}]_n$ .** A yellow block-like crystal was attached with Exxon Paratone N to a short length of fibre supported on a thin piece of copper wire inserted in a copper mounting pin. The crystal was quenched in a cold nitrogen gas stream from an Oxford Cryosystems Cryostream. A SuperNova Dual equipped with an Atlas detector and employing mirror monochromated  $\text{CuK}\alpha$  radiation from a micro-source was used for the data collection. Cell constants were obtained from a least squares refinement against 31217 reflections located between 8 and 153° 2 $\theta$ . Data were collected at 150.0(2) Kelvin with  $\omega$  scans to 153° 2 $\theta$ . The data processing was undertaken with CrysAlis Pro<sup>[36]</sup> and subsequent computations were carried out with WinGX<sup>[37]</sup> and ShelXle.<sup>[38]</sup> A multi-scan absorption correction was applied<sup>[36]</sup> to the data.

The structure was solved in the space group  $P21/c(\#14)$  by direct methods with SIR97<sup>[39-40]</sup> and extended and refined with SHELXL-2014/7.<sup>[41]</sup> The non-hydrogen atoms in the asymmetric unit were modelled with anisotropic displacement parameters and a riding atom model with group displacement parameters was used for the hydrogen atoms.

The structure contains large channels with disordered solvent molecules that were not fully resolved. Accordingly two models were refined; one included several partially occupied solvent sites, while the second used SQUEEZE<sup>[32]</sup> to accommodate the disordered solvent.

The model that included discrete solvent sites refined comparatively poorly with significant residual electron density that could not be satisfactorily assigned as discrete solvate or water molecule sites. Four partially occupied methanol solvent sites were included in the model, with occupancies totalling 1.075, together with a site treated as the oxygen atom of a partially occupied water site with an occupancy of 0.5. Hydrogen atoms were not included in the model for the solvent oxygen atoms. The conventional residual converged at 10.3% with a maximum residual electron density of  $3.6\text{e}/\text{\AA}^3$ . The use of SQUEEZE, without the inclusion of discrete solvent molecules, in the second model reduced the maximum residual density to  $1.86\text{e}/\text{\AA}^3$ , with a conventional residual of 6% and improved geometry. CIFs have been provided for both models. An ORTEP<sup>[42-43]</sup> depiction of the asymmetric unit of the model obtained with SQUEEZE, with 50% displacement ellipsoids, is provided in the ESI.

**$[\text{CuNPY}_3\text{NO}_3\cdot\text{solvent}]_n$ .** A yellow blade like crystal was attached with Exxon Paratone N to a nylon loop and quenched in a cold nitrogen gas stream from an Oxford Cryosystems Cryostream. An APEXII-FR591 diffractometer employing mirror monochromated  $\text{MoK}\alpha$  radiation generated from a rotating anode was used for the data collection. Cell constants were obtained from a least squares refinement against 9985 reflections located between 4 and 51° 2 $\theta$ . Data were collected at 100.0(2) Kelvin with  $\omega+\phi$  scans to 57° 2 $\theta$ . The data integration and reduction were undertaken with SAINT and XPREP,<sup>[44]</sup> and subsequent computations were carried out with the WinGX<sup>[37]</sup> and ShelXle<sup>[38]</sup> graphical user interfaces. An

empirical absorption correction determined with SADABS<sup>[45-46]</sup> was applied to the data.

The structure was solved in the space group *P2221*(#17) by direct methods with SHELXT<sup>[47]</sup> and extended and refined with SHELXL-2014/7.<sup>[41]</sup> In general, the non-hydrogen atoms in the asymmetric unit were modelled with anisotropic displacement parameters and a riding atom model with group displacement parameters was used for the hydrogen atoms.

The nitrate site occupancies were refined and then fixed at 0.5, and were modelled with isotropic displacement parameters. The structure contains large channels with disordered solvent molecules not fully resolved in difference maps. Accordingly two models were refined; one included partially occupied solvent sites, while the second did not include solvent sites and used SQUEEZE<sup>[32]</sup> to accommodate the disordered solvent. The model obtained using SQUEEZE is preferred, with better residuals and geometrical precision.

An ORTEP<sup>[42-43]</sup> depiction of the asymmetric unit complex molecule with 50% displacement ellipsoids is provided in the ESI. The absolute structure was established with the Flack parameter<sup>[48-52]</sup> refining to 0.063(17); there appears to be a minor inversion twin component.

## Physical Characterisation

**General details.** Thermal gravimetric analysis was performed under a flow of nitrogen (0.1 L/min) on a TA Instruments Hi-Res or Discovery Thermogravimetric Analyser from 25–600 °C at 1 °C/min. Powder X-ray diffraction (PXRD) data were obtained on a PANalytical X'Pert PRO Diffractometer producing Cu $\alpha$  (1.5406 Å) radiation, where the sample was lightly ground prior to analysis.

**Solid State UV/Vis/NIR.** UV/Vis/NIR spectroscopy was performed on a Cary 5000 Spectrophotometer equipped with a Harrick Praying Mantis accessory, where dried BaSO<sub>4</sub> was used for the baseline. Spectra are reported as the Kubelka-Munk transform, where  $F(R) = (1-R)^2/2R$  ( $R$  is the diffuse reflectance of the sample as compared to BaSO<sub>4</sub>).

**Solid State Electrochemistry.** Solid state electrochemical measurements were performed using a Bioanalytical Systems Epsilon Electrochemical Analyser. Argon was bubbled through solutions of 0.1 M [(*n*-C<sub>4</sub>H<sub>9</sub>)<sub>4</sub>N]PF<sub>6</sub>/CH<sub>3</sub>CN. The cyclic voltammograms (CVs) were recorded using a glassy carbon working electrode (1.5 mm diameter), a platinum wire auxiliary electrode and an Ag/Ag<sup>+</sup> wire quasi-reference electrode. Solid state samples were mounted on the glassy carbon working electrode by dipping the electrode into a paste made of the powder sample in acetonitrile. Ferrocene was added as an internal standard upon completion of each experiment. All potentials are quoted versus Fc/Fc<sup>+</sup>.

**Solid State Spectroelectrochemistry (Vis/NIR).** In the solid state, the diffuse reflectance spectra of the electrogenerated species were collected *in situ* in a 0.1 M [(*n*-C<sub>4</sub>H<sub>9</sub>)<sub>4</sub>N]PF<sub>6</sub>/CH<sub>3</sub>CN electrolyte over the range 5000–25000 cm<sup>-1</sup> using a Harrick Omni Diff Probe attachment and a custom

built solid state spectroelectrochemical cell described previously.<sup>[35]</sup> The cell consisted of a Pt wire counter electrode and a Ag/Ag<sup>+</sup> quasi-reference electrode. The solid sample was immobilised onto a 0.1 mm thick Indium-Tin-Oxide (ITO) coated quartz slide (which acted as the working electrode) using a thin strip of Teflon tape. The applied potential (from 0 to 1.5 V) was controlled using an eDAQ potentiostat. Continuous scans of the sample were taken and the potential increased gradually until a change in the spectrum was observed.

## Acknowledgements

We gratefully acknowledge support from the Australian Research Council.

## Notes and references

<sup>a</sup> School of Chemistry, The University of Sydney, New South Wales 2006, Australia. Fax: +61 (2) 9351 3329; Tel: +61 (2) 9351 3777; E-mail: [deanna.dalessandro@sydney.edu.au](mailto:deanna.dalessandro@sydney.edu.au)

† [*CuNP<sub>3</sub>Cl*.solvent]<sub>n</sub> Formula C<sub>33</sub>H<sub>24</sub>ClCuN<sub>4</sub>, *M* 575.55, monoclinic, space group *P21/c*(#14), *a* 10.05130(10), *b* 28.1929(2), *c* 12.21890(10) Å, *b* 112.2430(10), *V* 3204.88(5) Å<sup>3</sup>, *D<sub>c</sub>* 1.193 g cm<sup>-3</sup>, *Z* 4, crystal size 0.201 by 0.108 by 0.056 mm, colour yellow, habit block, temperature 150.0(2) Kelvin, *l*(Cu K $\alpha$ ) 1.5418 Å, *m*(Cu K $\alpha$ ) 1.992 mm<sup>-1</sup>, *T*(CRYALISPRO, AGILENT TECHNOLOGIES) min,max 0.818, 1.00, *2 $\theta$* max 153.19, *hkl* range -12 12, -35 35, -15 14, *N* 62752, *N*ind 6714(*R*merge 0.0263), *N*obs 6371(*I* > 2 $\sigma$ (*I*)), *N*var 352, residuals\* *R1*(*F*) 0.0592, *wR2*(*F2*) 0.1787, *GoF*(all) 1.047, *D<sub>r</sub>*min,max -0.821, 1.859 e<sup>-</sup> Å<sup>-3</sup>.

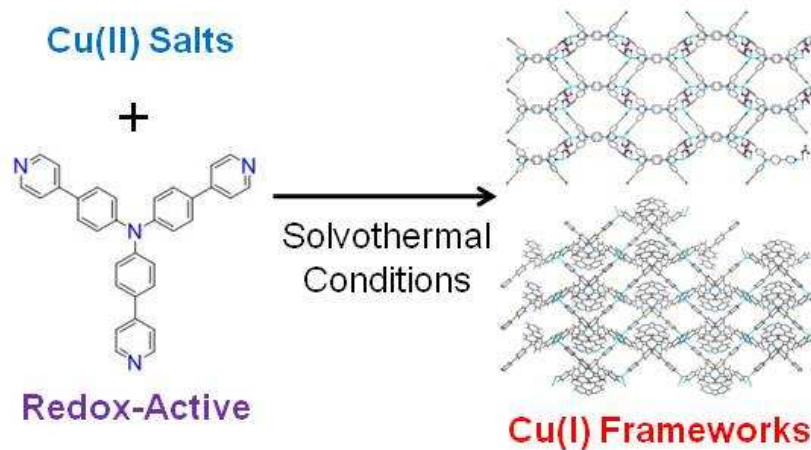
[*CuNP<sub>3</sub>NO<sub>3</sub>*.solvent]<sub>n</sub> Model Formula C<sub>33</sub>H<sub>24</sub>CuN<sub>5</sub>O<sub>3</sub>, *M* 602.11, orthorhombic, space group *P2221*(#17), *a* 9.0770(16), *b* 13.831(2), *c* 32.773(6) Å, *V* 4114.4(12) Å<sup>3</sup>, *D<sub>c</sub>* 0.972 g cm<sup>-3</sup>, *Z* 4, crystal size 0.149 by 0.098 by 0.051 mm, colour yellow, habit balde, temperature 100.0(2) Kelvin, *l*(MoK $\alpha$ ) 0.71073 Å, *μ*(MoK $\alpha$ ) 0.561 mm<sup>-1</sup>, *T*(SADABS)min,max 0.767, 0.862, *2 $\theta$* max 56.73, *hkl* range -12 12, -18 18, -43 43, *N* 69365, *N*ind 10282(*R*merge 0.0754), *N*obs 8019(*I* > 2 $\sigma$ (*I*)), *N*var 364, residuals\* *R1*(*F*) 0.0540, *wR2*(*F2*) 0.1383, *GoF*(all) 1.104,  $\Delta\rho$ min,max -0.569, 0.751 e<sup>-</sup> Å<sup>-3</sup>.

CCDC (1055957, 1055958, 1055959, 1055960) contains the supplementary crystallographic data for this paper. These data can be obtained free of charge via [www.ccdc.cam.ac.uk/data\\_request/cif](http://www.ccdc.cam.ac.uk/data_request/cif), or by emailing [data\\_request@ccdc.cam.ac.uk](mailto:data_request@ccdc.cam.ac.uk), or by contacting The Cambridge Crystallographic Data Centre, 12 Union Road, Cambridge CB2 1EZ, UK; fax: +44 1223 336033.

Electronic Supplementary Information (ESI) available: X-ray crystallographic files in CIF format for disordered solvent and squeezed structures, table of crystallographic information, powder X-ray diffraction, TGA and infrared spectra. See DOI: 10.1039/b000000x/

1. C. Hua, A. Rawal, T. B. Faust, P. D. Southon, R. Babarao, J. M. Hook, D. M. D'Alessandro, *J. Mater. Chem. A* 2014, **2**, 12466.

2. S. Qiu, G. Zhu, *Coord. Chem. Rev.* 2009, **253**, 2891.
3. H.-L. Jiang, Q. Xu, *Chem. Commun.* 2011, **47**, 3351.
4. F. J. Rizzuto, T. B. Faust, B. Chan, C. Hua, D. M. D'Alessandro, C. J. Kepert, *Chem. Eur. J.* 2014, **20**, 17597.
5. C. F. Leong, T. B. Faust, P. Turner, P. M. Usov, C. J. Kepert, R. Babarao, A. W. Thornton, D. M. D'Alessandro, *Dalton Trans.* 2013, **42**, 9831.
6. C. F. Leong, B. Chan, T. B. Faust, P. Turner, D. M. D'Alessandro, *Inorg. Chem.* 2013, **52**, 14246.
7. C. F. Leong, B. Chan, T. B. Faust, D. M. D'Alessandro, *Chem. Sci.* 2014, **5**, 4724.
8. C. Hua, P. Turner, D. M. D'Alessandro, *Dalton Trans.* 2013, **42**, 6310.
9. C. Hua, D. M. D'Alessandro, *CrystEngComm* 2014, **16**, 6331.
10. J. E. Halls, D. Jiang, A. D. Burrows, M. A. Kulandainathan, F. Marken, in *Electrochemistry: Volume 12, Vol. 12*, The Royal Society of Chemistry, **2014**, pp. 187.
11. V. Martínez, A. B. Gaspar, M. C. Muñoz, R. Ballesteros, N. Ortega-Villar, V. M. Ugalde-Saldivar, R. Moreno-Esparza, J. A. Real, *Eur. J. Inorg. Chem.* 2009, **2009**, 303.
12. A. A. Talin, A. Centrone, A. C. Ford, M. E. Foster, V. Stavila, P. Haney, R. A. Kinney, V. Szalai, F. El Gabaly, H. P. Yoon, F. Léonard, M. D. Allendorf, *Science* 2014, **343**, 66.
13. J. E. Halls, S. D. Ahn, D. Jiang, L. L. Keenan, A. D. Burrows, F. Marken, *J. Electroanal. Chem.* 2013, **689**, 168.
14. I. Hod, W. Bury, D. M. Gardner, P. Deria, V. Roznyatovskiy, M. R. Wasielewski, O. K. Farha, J. T. Hupp, *J. Phys. Chem. Lett.* 2015, **6**, 586.
15. Y. Lu, M. Tonigold, B. Bredenkötter, D. Volkmer, J. Hitzbleck, G. Langstein, *Z. Anorg. Allg. Chem.* 2008, **634**, 2411.
16. M. Tonigold, Y. Lu, A. Mavrandonakis, A. Puls, R. Staudt, J. Möllmer, J. Sauer, D. Volkmer, *Chem. Eur. J.* 2011, **17**, 8671.
17. Y. E. Cheon, M. P. Suh, *Angew. Chem. Int. Ed.* 2009, **48**, 2899.
18. H. R. Moon, J. H. Kim, M. P. Suh, *Angew. Chem. Int. Ed.* 2005, **44**, 1261.
19. F. Meng, M. Zhang, K. Shen, Y. Li, H. Zheng, *Dalton Trans.* 2015, **44**, 1412.
20. J.-S. Hu, Z. Lei, C.-L. Pan, J. He, *Mendeleev Commun.* 2014, **24**, 290.
21. M.-D. Zhang, C.-M. Di, L. Qin, X.-Q. Yao, Y.-Z. Li, Z.-J. Guo, H.-G. Zheng, *Cryst. Growth Des.* 2012, **12**, 3957.
22. F. Meng, L. Qin, M. Zhang, H. Zheng, *CrystEngComm* 2014, **16**, 698.
23. M.-D. Zhang, C.-M. Di, L. Qin, Q.-X. Yang, Y.-Z. Li, Z.-J. Guo, H.-G. Zheng, *CrystEngComm* 2013, **15**, 227.
24. S. M. F. Lo, S. S. Y. Chui, L.-Y. Shek, Z. Lin, X. X. Zhang, G.-h. Wen, I. D. Williams, *J. Am. Chem. Soc.* 2000, **122**, 6293.
25. O. M. Yaghi, H. Li, *J. Am. Chem. Soc.* 1995, **117**, 10401.
26. A. N. Parvulescu, G. Marin, K. Suwinska, V. C. Kravtsov, M. Andruh, V. Parvulescu, V. I. Parvulescu, *J. Mater. Chem.* 2005, **15**, 4234.
27. P. Amo-Ochoa, G. Givaja, P. J. S. Miguel, O. Castillo, F. Zamora, *Inorg. Chem. Commun.* 2007, **10**, 921.
28. J.-K. Cheng, Y.-G. Yao, J. Zhang, Z.-J. Li, Z.-W. Cai, X.-Y. Zhang, Z.-N. Chen, Y.-B. Chen, Y. Kang, Y.-Y. Qin, Y.-H. Wen, *J. Am. Chem. Soc.* 2004, **126**, 7796.
29. J. Tao, X. Yin, R. Huang, L. Zheng, *Inorg. Chem. Commun.* 2002, **5**, 1000.
30. F. R. Allen, *Acta Crystallogr., Sect. B: Struct. Sci.* 2002, **58**, 380.
31. C. Lambert, G. Nöll, *J. Am. Chem. Soc.* 1999, **121**, 8434.
32. A. L. Spek, *J. Appl. Crystallogr.* 2003, **36**, 7.
33. G. W. F. Albert Cotton, *Advanced Inorganic Chemistry, A Comprehensive Text*, Third ed., Interscience Publishers, Canada, 1972.
34. S. Amthor, B. Noller, C. Lambert, *Chem. Phys.* 2005, **316**, 141.
35. P. M. Usov, C. Fabian, D. M. D'Alessandro, *Chem. Commun.* 2012, **48**, 3945.
36. CrysAlisPro, Yarnton, Oxfordshire. OX5 1QU, UK.
37. L. Farrugia, *J. Appl. Crystallogr.* 1999, **32**, 837.
38. C. B. Hübschle, G. M. Sheldrick, B. Dittrich, *J. Appl. Crystallogr.* 2011, **44**, 1281.
39. A. Altomare, G. Cascarano, C. Giacovazzo, A. Guagliardi, M. C. Burla, G. Polidori, M. Camalli, *J. Appl. Crystallogr.* 1994, **27**, 435.
40. A. Altomare, M. C. Burla, M. Camalli, G. L. Cascarano, C. Giacovazzo, A. Guagliardi, A. G. G. Moliterni, G. Polidori, R. Spagna, *J. Appl. Crystallogr.* 1998, **32**, 115.
41. G. M. Sheldrick, *SHELXTL reference manual: Version 5*, Analytical X-ray Instruments Inc., Madison, Wisconsin, USA, 1996.
42. M. N. Burnett, C. K. Johnson, Oak Ridge National Laboratory, Tennessee, USA, **1996**.
43. L. J. Farrugia, *J. Appl. Crystallogr.* 1997, **30**, 565.
44. Bruker (2014); *SMART, SAINT and XPREP. Area detector control and data integration and reduction software. Bruker Analytical X-ray Instruments Inc.*, Madison, Wisconsin, USA, **2014**
45. L. Krause, R. Herbst-Irmer, G. M. Sheldrick, D. Stalke, *J. Appl. Crystallogr.* 2015, **48**, 3.
46. R. H. Blessing, *Acta Crystallogr., Sect. A: Found. Crystallogr.* 1995, **A51**, 33.
47. G. M. Sheldrick, *Acta Crystallogr., Sect. A: Found. Crystallogr.* 2015, **A71**, 3.
48. H. D. Flack, *Acta Crystallogr., Sect. A: Found. Crystallogr.* 1983, **39**, 876.
49. G. Bernardinelli, *Acta Crystallogr., Sect. A: Found. Crystallogr.* 1985, **41**, 500.
50. H. D. Flack, G. Bernardinelli, *Acta Crystallographica Section A* 1999, **55**, 908.
51. H. D. Flack, G. Bernardinelli, *J. Appl. Crystallogr.* 2000, **33**, 1143.
52. S. Parsons, H. D. Flack, T. Wagner, *Acta Crystallographica Section B* 2013, **69**, 249.



Two Cu(I) frameworks were synthesised with the NPy<sub>3</sub> ligand and Cu(II) salts to yield electroactive Cu(I) frameworks whose spectral properties varied as a function of the redox state.